Disease progression patterns of brain morphology in schizophrenia: More progressed stages in treatment-resistance

shinichiro nakajima (shinichiro.l.nakajima@gmail.com)
Keio University, School of Medicine https://orcid.org/0000-0002-2601-2195
Daichi Sone
Jikei University School of Medicine https://orcid.org/0000-0001-9617-706X
Alexandra Young
Shunichiro Shinagawa
Sakiko Tsugawa
Keio University School of Medicine https://orcid.org/0000-0001-9974-316X
Yusuke Iwata
Centre for Addiction and Mental Health
Ryosuke Tarumi
Keio University School of Medicine
Kamiyu Ogyu
Keio University School of Medicine
Shiori Honda
Keio University School of Medicine
Ryo Ochi
Karin Matsushita
Fumihiko Ueno
Centre for Addiction and Mental Health
Nobuaki Hondo
Keio University School of Medicine
Akihiro Koreki
Edgardo Torres-Carmona
Wanna Mar
Centre for Addiction and Mental Health
Nathan Chan
https://orcid.org/0000-0001-7516-1616
Teruki Koizumi
Hideo Kato
Keisuke Kusudo
Vincenzo De Luca

Centre for Addiction and Mental Health Toronto
Philip Gerretsen
Centre for Addiction and Mental Health
Gary Remington
Mitsumoto Onaya
Yoshihiro Noda
Keio University School of Medicine https://orcid.org/0000-0002-2155-0357
Hiroyuki Uchida
Keio University School of Medicine https://orcid.org/0000-0002-0628-7036
Masaru Mimura
Masahiro Shigeta
Ariel Graff-Guerrero
Centre for Addiction and Mental Health

Article

Keywords:

Posted Date: February 8th, 2023

DOI: https://doi.org/10.21203/rs.3.rs-2523052/v1

Abstract

Given the heterogeneity and possible disease progression in schizophrenia, identifying the neurobiological subtypes and progression patterns in each patient may lead to the development of clinically useful biomarkers. In this cross-sectional study, we adopted data-driven machine-learning techniques to classify and stage the progression patterns of brain morphological changes in schizophrenia and investigate the association with treatment resistance. We included 177 patients with schizophrenia, characterized by treatment response or resistance, with 3D T1-weighted magnetic resonance imaging from 3 institutions. Cortical thickness and subcortical volumes calculated by FreeSurfer were converted into Z-scores using 73 healthy controls data. The Subtype and Stage Inference (SuStaIn) algorithm was used for unsupervised machine-learning classification and staging. As a result, SuStaIn identified three different subtypes: 1) subcortical volume reduction (SC) type (73 patients, 47.4%), in which volume reduction of subcortical structures occurs first and moderate cortical thinning follows, 2) globus pallidus hypertrophy and cortical thinning (GP-CX) type (42 patients, 27.3%), in which globus pallidus hypertrophy initially occurs followed by progressive cortical thinning, 3) cortical thinning (pure CX) type (39 patients, 25.3%), in which thinning of the insular and lateral temporal lobe cortices primarily happens. The remaining 23 patients were assigned to baseline stage of progression (no change). SuStaIn also found 84 stages of progression, and treatment-resistant schizophrenia showed significantly more progressed stages of progression than treatment-responsive cases (p=0.001). The GP-CX type presented in earlier stages than the pure CX type (p=0.009). In conclusion, the brain morphological progressions in schizophrenia can be classified into three subtypes by SuStaIn algorithm. Treatment resistance was associated with more progressed stages of the disease, which may suggest a novel biomarker for schizophrenia.

Introduction

Schizophrenia is a common psychiatric disorder presenting with psychotic symptoms as well as negative and cognitive symptoms [1]. Despite longstanding and continuous efforts, we have not identified any distinct pathophysiology or established objective biomarkers in schizophrenia. While the diagnosis of schizophrenia is still based on psychiatric symptoms, patients with schizophrenia often show heterogeneous symptoms and treatment response[2, 3], calling into question whether it represents a single disease, particularly in terms of neurotransmitter systems[4]. In addition to symptom heterogeneity, treatment response is also diverse. For example, treatment-resistant schizophrenia (TRS) defines a distinct subpopulation showing poor response to conventional pharmacological treatment[5] and, as a result, a form of the illness associated with serious social and economic burden[6]. The neurobiological basis of TRS remains to be elucidated, despite numerous strategies including neuroimaging studies[7–9].

To address this disease heterogeneity, studies have proposed schizophrenia subtypes based on symptoms[10, 11] as well as brain structures[12]. In the latter, for example, each individual's brain structural abnormality is categorized into two distinct subtypes by machine learning; however, to date such brain

morphological subtypes have shown little relationship with clinical symptoms[12]. In employing such a strategy, it is important to acknowledge that such brain morphological abnormalities may be progressive and involve cortical thinning in the temporal or frontal lobes[13, 14]. TRS has been associated with longer duration of untreated psychosis[15, 16], raising the possibility that TRS may be caused by more disease progression.

In light of the above, categorization that incorporates staging may prove valuable in our understanding of treatment resistance in schizophrenia. In this regard, machine learning analysis has been increasingly applied to uncovering patterns in clinical parameters that may translate to personalized, more reliable biomarkers[17, 18]. Subtype and Stage Inference (SuStaIn) is an unsupervised machine learning algorithm to uncover data-driven disease phenotypes with temporal progression patterns, and it has been widely utilized to identify disease subtypes and stages[19–22].

Here, we applied the SuStaIn algorithm to classify disease progression patterns and staging of brain morphology in schizophrenia, with the goal of identifying distinct biological subtypes in the context of illness progression and associations with clinical measures. We hypothesized that TRS may be associated with more progressed disease staging; in addition, we investigated the consistency of anatomical subtype categorizations with previously published data[12] as well as relationship with other clinical characteristics.

Materials And Methods

Participants

We analyzed international. multi-center cross-sectional neuroimaging data comprising 177 patients with schizophrenia and 73 healthy controls (HCs): 54 patients with schizophrenia (24 TRS, 30 non-TRS) and 28 HCs from Komagino hospital[23], Tokyo, Japan, 70 patients with schizophrenia (49 TRS, 21 non-TRS) from the Centre for Addiction and Mental Health (CAMH)[24], Toronto, Canada, and 53 patients with schizophrenia (23 TRS, 30 non-TRS) from Shimofusa Psychiatric Medical Center, Chiba, Japan (Table 1). In each cohort, there were no significant differences in age and sex between the schizophrenia and HC groups.

Table 1
Demographics and subtype/staging of participants from the three institutes.

	Cohort 1 (Komagino)	Cohort 2 (Toronto)	Cohort 3 (Shimofusa)
HC	N = 28	N = 21	N = 24
Age (yrs)	46.0 (18) †	36.0 (23) †	41.5 (18) †
Sex (M:F)	12:16 ‡	15:6 ‡	14:10 ‡
Schizophrenia	N = 54	N = 70	N = 53
Age (yrs)	43.5 (17) †	46.5 (22) †	39.0 (17) †
Sex (M:F)	24:30 ‡	53:17 ‡	29:24 ‡
TRS (N)	24	49	23
Onset (yrs)	25.0 (11)	23.0 (9)	20.0 (10)
Duration (yrs)	14.0 (15.5)	20.0 (20.3) *	15.0 (17.5)
Education (yrs)	12.0 (3)	12.5 (2) *	12.0 (3)
Antipsychotics (CP)	600 (500)	493.75 (300) *	450 (570)
PANSS-P	14.5 (17)	13.0 (10) *	17.0 (10)
PANSS-N	22.0 (17)	17.5 (5) *	18.0 (8)
PANSS-G	30.5 (29)	32.5 (11) *	36.0 (16)
PANSS-T	67.5 (65)	65.0 (24) *	70.0 (26)
Subtypes	SC = 15, GP-CX = 19, pure CX = 8, stage-0 = 12	SC = 31, GP-CX = 13, pure CX = 20, stage-0 = 6	SC = 27, GP-CX = 10, pure CX = 11, stage-0 = 5
Staging	5.0 (9)	7.0 (11)	6.0 (10)

Continuous variables are shown as median (IQR).

* missing in 4 patients.

† No significant differences between HC and Schizophrenia in each cohort (p = 0.395, 0.072, 0.656, respectively, Mann-Whitney U tests).

‡ No significant differences between HC and Schizophrenia in each cohort (p = 0.891, 0.692, 0.767, respectively, $\chi 2$ tests).

Participants partly overlapped with previous studies in which the same inclusion/exclusion criteria and clinical evaluations were used[9, 23–27]. Patients were diagnosed with schizophrenia based on the

Diagnostic and Statistical Manual of Mental Disorders 4th Ed (DSM-IV)[28]. The Positive and Negative Syndrome Scale (PANSS)[29] and the Clinical Global Impression Severity Scale (CGI-S)[30] were used for assessment of clinical symptoms. TRS was determined by the modified Treatment Response and Resistance in Psychosis (TRRIP) Working Group Consensus criteria[31]. Treatment response was defined by (i) CGI-S score ≤ 3, (ii) PANSS positive symptom item scores ≤ 3, and (iii) no symptomatic relapse in the previous 3 months. In contrast, inadequate treatment response was defined by (i) CGI-S score ≥ 4, and (ii) ≥ 4 on at least 2 PANSS positive symptom items after adequate antipsychotic trials. Response to past antipsychotic trials was determined based on medical records. We also confirmed no history of psychiatric illness in HCs by using the Mini-International Neuropsychiatric Interview (MINI)[32]. The following exclusion criteria were applied to all participants: (i) substance abuse or dependance within the past six months; (ii) positive urine drug screen at inclusion or before the MRI scan; (iii) history of head trauma resulting in unconsciousness for > 30min; or (iv) an unstable physical illness or neurological disorder.

All participants provided written informed consent, and the study protocol was approved by the Ethics committees at each institute.

MRI acquisition and preprocessing

Participants underwent 3D T1-weighted structural MRI scans on the following protocols: (i) at the Komagino Hospital, 3 T Signa HDxt scanner (GE Healthcare) with an eight-channel head coil (BRAVO, echo time [TE] = 2.8 ms, repetition time [TR] = 6.4 ms, inversion time [TI] = 650 ms, flip angle = 8◦, field of view [FOV] = 230 mm, matrix size = 256 × 256, slice thickness = 0.9 mm), (ii) at the Centre for Addiction and Mental Health, a 3 T GE Discovery R750 scanner (GE Healthcare) with an eight-channel head coil (BRAVO, TE = 3 ms, TR = 6.74 ms, TI = 650 ms, flip angle = 8◦, FOV = 230 mm, matrix size = 256 × 256, slice thickness = 0.9 mm), (iii) at the Shimofusa Psychiatric Medical Center, a 1.5 T Signa Explorer (GE Healthcare) with a 12-channel head coil (FSPGR, TE = 5.1ms, TR = 12.2ms, TI = 913ms, flip angle = 25◦, FOV = 256mm, matrix size = 256x256, slice thickness = 1.0mm).

We used FreeSurfer software (v.6.0, https://surfer.nmr.mgh.harvard.edu) to calculate cortical thickness (CT) and subcortical gray matter (GM) volumes of the whole cerebrum as well as the intracranial volumes (ICV) based on the 3D T1-weighted images of all the participants. Image processing included the removal of non-brain tissues with a hybrid watershed/surface deformation procedure, automated Talairach transformation, and segmentation of the subcortical structure and cortex based on the Desikan-Killiany Atlas. We confirmed segmentation accuracy in all subjects with visual inspection.

Subtype and Stage Inference (SuStaIn) analysis

Firstly, the subcortical GM volumes were corrected for individual's ICV, and then all CT and subcortical GM volumes were corrected for age and sex. As SuStaIn uses Z-scores for the machine learning analysis[19], we calculated Z-scores for each cohort. In other words, Z-score calculations were performed using each HC cohort with the same scanner and protocol at each institute.

It is also necessary to select the relevant regions of interest (ROIs) for obtaining reliable results by machine learning; we chose all ROIs with significant changes in the multi-center mega analysis by ENIGMA consortium[33, 34], one of the most reliable strategies in evaluating brain morphological alteration in schizophrenia. The detailed list of 28 identified ROIs is shown in Supplementary Table S1. Since globus pallidus (GP) may show increased volumes[33], we converted the Z-score of GP by multiplying (-1) to reflect hypertrophy, while the Z-score of the other ROIs represented cortical thinning or GM volume loss.

Finally, the Z-scores of the 28 ROIs for the 177 patients with schizophrenia were entered into the SuStaIn algorithm (https://github.com/ucl-pond/SuStaInMatlab). As SuStaIn represents an unsupervised machine learning strategy, any other information than the Z-scores, e.g., the anatomy of each ROI or clinical data, were not taken into account. The linear Z-score model and mathematical model underlying the SuStaIn algorithm are described in the previous study[19]; steps included model-fitting, convergence, uncertainty estimation, cross-validation, and similarity between subtypes. As described previously[19, 21, 22], SuStaIn categorized individuals into subtypes and estimated the most likely sequence in which selected ROIs reach different progression stages over time.

Statistical analysis

Statistical analyses were performed by SPSS (IBM Corp. Version 25.0. Armonk, NY: IBM Corp). Parametric or non-parametric distributions of variables were examined by Shapiro-Wilk test, and the null hypothesis of normal distribution was rejected in all the clinical variables in this study. On the other hand, the corrected CT and subcortical GM volumes in HCs were normally distributed, which should justify the conversion process to Z-score for SuStaIn.

As a primary analysis, we investigated the relationships of TRS with disease subtypes or staging derived from the SuStaIn analysis. The categorical relationship, i.e., TRS/non-TRS vs. disease subtypes, was analyzed by $\chi 2$ test, and the estimated stages between TRS and non-TRS were compared by Mann-Whitney U test. For more exploratory analyses, we examined the association of the subtypes and staging with other clinical characteristics, including onset age, disease duration, medication dose, or PANSS scores. Among the subtypes, continuous variables were compared by Kruskal-Wallis tests, while $\chi 2$ tests were used for categorical variables. Regarding the staging, Spearman's rank correlation tests were used to reveal relationships with other variables. A $p < 0.05$ was considered as statistically significant.

Validation for reproducibility

To confirm the reproducibility of the subtype and staging categorization, we repeated the SuStaIn analysis in each cohort separately. The subtypes and staging results from each additional analysis were compared with the main original results from all the patients, using $\chi 2$ test and Spearman's rank correlation test.

Results

Estimated subtypes, stages, and treatment-resistance

SuStaIn identified three different subtypes of brain morphological changes in schizophrenia (Fig. 1) i.e., i) subcortical volume reduction (SC) type (73 patients), ii) globus pallidus hypertrophy and cortical thinning (GP-CX) type (42 patients), iii) cortical thinning (pure CX) type (39 patients). In the SC type, subcortical volume loss, particularly the hippocampi and thalami, initially occurs and cortical thinning follows (left in Fig. 1). In the GP-CX type, the globus pallidus hypertrophy initially happens, followed by cortical thinning with no severe atrophy of other subcortical structures (middle in Fig. 1). In the pure CX type, cortical thinning, particularly in the lateral temporal and insular cortices, mainly occurs and subcortical volumes are not severely affected (right in Fig. 1). The remaining 23 patients were assigned to baseline stage of progression (no change) and not categorized into any subtypes.

SuStaIn also found 84 stages of progression (Fig. 1). The histograms of disease stages of each participant in the TRS and non-TRS groups are presented in Fig. 2. The TRS group showed significantly more progressed disease stages than non-TRS ($p = 0.001$, Mann-Whitney U test). With regard to subtype results, GP-CX type showed significantly less progressed stages than pure CX type ($p = 0.009$), and a similar trend was found in comparison to SC type (Table 2) although there was no direct association of subtypes with TRS.

Table 2
Clinical features among the three subtypes derived from SuStaIn analysis.

	SC type (N = 73)	GP-CX type (N = 42)	pure CX type (N = 39)	p-val.
Age (yrs)	44.0 (22)	40.0 (20)	44.0 (14)	0.870†
Sex (M:F)	48:25	24:18	21:18	0.415††
TRS (N)	41	23	22	0.986††
Onset (yrs)	21.0 (13) *	24.0 (8) **	23.0 (8)	0.950†
Duration (yrs)	15.0 (20) *	19.0 (15.5) **	19.0 (18)	0.673†
Education (yrs)	12.0 (2) *	12.0 (4) **	12.0 (2)	0.480†
Antipsychotics (CP)	474 (430.5) *	581.25 (467) **	450 (375)	0.419†
PANSS-P	15.0 (11) *	14.0 (16) **	14.0 (14)	0.862†
PANSS-N	18.5 (9) *	19.0 (13) **	18.0 (12)	0.852†
PANSS-G	35.0 (15) *	32.0 (20) **	32.0 (18)	0.662†
PANSS-T	69.0 (28) *	67.0 (48) **	68.0 (43)	0.755†
Staging	8.0 (14)	6.0 (7) †††	10.0 (11)	0.010†
Continuous variables are shown as median (IQR).				
* Missing in 2 patients				
** Missing in 1 patient				
† Kruskal-Wallis test				
†† $\chi 2$ test				
††† Significantly lower than pure CX type (p = 0.009, post-hoc Dunn test with Bonferroni correction) and a trend toward lower than SC type (p = 0.076). No significance between pure CX and SC types (p = 0.766).				

Associations with other clinical characteristics

As shown in Table 2, there were no significant relationships between the three subtypes and other clinical characteristics. The proportion of TRS also did not significantly differ across the three subtypes (Table 2). Of 23 patients in the baseline stage, 10 subjects (43%) were TRS. In addition, the estimated stages were

not correlated with most of other clinical variables except for the PANSS positive and total scores (uncorrected $p < 0.05$, Table 3).

Table 3
Correlation analysis with the estimated stage of disease progression.

	Spearman's rs	p-val.
Age	0.010	0.900
Sex (M = 1, F = 2)	-0.024	0.749
Onset	0.084	0.270
Duration	0.009	0.905
Education	-0.056	0.455
Antipsychotics	0.116	0.124
PANSS-P	**0.175**	**0.021**
PANSS-N	0.105	0.171
PANSS-G	0.129	0.091
PANSS-T	**0.154**	**0.043**
Bold font denotes uncorrected $p < 0.05$.		

Reproducibility analysis

The results of the reproducibility analysis are shown in Fig. 3. Although the subtype patterns were generally consistent with the main analysis, SuStaIn did not identify a pure CX type in cohort 2 (Fig. 3-A). Therefore, 18 of 20 patients in cohort 2 with pure CX type in the main analysis were classified into GP-CX type (Fig. 3-B). Otherwise, patients were categorized into the same subtype groups ($p < 10^{-43}$, $\chi 2$ test). The stage of disease progression was well reproduced (Spearman's rs = 0.985, $p < 10^{-134}$, Fig. 3-C).

Discussion

The current study applied the unsupervised machine learning model to data of brain morphology in patients with schizophrenia and identified three subtypes with the following progression patterns: SC type, in which subcortical volume loss is more dominant; GP-CX type, in which GP increase initially occurs and cortical thinning follows; and, pure CX type, in which cortical thinning mainly occurs. Furthermore, more patients with TRS were at the progressed disease stages compared to those with non-TRS. Additionally, GP-CX type was associated with less progressive stages. These brain morphological subtypes and staging may, in turn, lead to the development of clinically useful individualized biomarkers.

There have been various attempts to identify subtypes and staging in neurodegenerative diseases by SuStaIn. In frontotemporal dementia, four distinct subtypes with progression patterns were detected using structural MRI, which were consistent with genetic variance[19]. Another study applied SuStaIn to tau-PET images of Alzheimer's disease and identified four distinct spatiotemporal trajectories of progression[21]. In the present study, we applied SuStaIn to schizophrenia and found three subtypes with distinct features in terms of anatomical patterns. SuStaIn represents an unsupervised algorithm, and the neuroanatomical information of each ROI and other clinical data were not incorporated into the analysis. Nevertheless, the three subtypes were anatomically consistent; cortical and subcortical patterns could be separated and the left/right sides generally changed simultaneously (Fig. 1). Such anatomical consistency would support the validity of the SuStaIn classification.

In a previous study by machine learning and structural MRI in schizophrenia, two distinct patterns were reported: i.e., (1) widespread GM volume loss in the frontotemporal and insular cortices, thalamus, and nucleas accumbens, and (2) increased subcortical GM volumes with no distinct cortical GM loss[12]. These findings may partly align with our results in terms of classification into cortical and subcortical patterns. However, given the possible progression of schizophrenia, incorporating disease staging may be desirable. Our results also advance the field incorporating subpopulation data (i.e. TRS and non-TRS) that seems linked to different neurobiological dysfunction[4, 35]. Among the identified three subtypes, the SC type showed initial subcortical GM loss and subsequent cortical thinning, whereas both the GP-CX and the pure CX types presented earlier and with more distinct cortical thinning and less evident subcortical GM decrease than the SC type (Fig. 1). The clear difference between the GP-CX and pure CX types was the initial GP volume increase. GP increase in patients with schizophrenia has been consistently reported by multi-center studies at a group-level comparison with HCs[33, 36]. Although no direct associations with TRS were found, the GP-CX type showed less disease progression than the pure CX type. On the other hand, in the reproducibility analysis, it was difficult to distinguish between GP-CX and pure CX in a smaller cohort (cohort 2, Fig. 3); accordingly, more careful interpretation may be needed. At any rate, the pathological meaning of GP increase in schizophrenia is not well understood, and further investigation is needed to interpret our current model.

Several studies have investigated the neurobiological mechanism of TRS, including involvement of glutamate and GABA systems[23, 24, 27, 37, 38] as well as cortical abnormality patterns[9, 25]. In the current study, stage progression was associated with TRS but not with disease duration (Table 3). Thus, it does not appear that the disease simply progresses as time progresses. To this point, longer duration of untreated psychosis and treatment non-adherence have been identified as associated factors with TRS[16]. The point has also been made that TRS is associated with central oxidative stress and increased variability of glutathione[39]. Together with our findings, such unfavorable factors may advance the disease stages and pathological changes in TRS. These different influences may, in fact, contribute to the variable outcomes associated with TRS e.g., clozapine response.

The strengths of this study include a novel data-driven approach for individualized subtyping and staging, findings of a significant association between progressed staging and treatment-resistance, and the reproducibility of multi-site data. On the other hand, this study has several limitations. First, it is difficult to demonstrate the validity of current results in the absence of a well-established gold standard. One possible solution is to longitudinally follow these cohorts to confirm whether established subtypes follow specific trajectories. Selection of ROIs may also raise some controversy although we adopted the most reliable evidence from the international mega-analyses[33, 34]. In addition, we did not find any relationships between subtypes and clinical characteristics; however, this issue is consistent with the previous study[12]. We speculate that this reflects the limitations of diagnoses based solely on symptoms and the assessment of disease status only by scoring. Much more knowledge related to neurobiological mechanisms may serve to address this limitation. Other limitations include sample size, cross-sectional design, and potential effects of medications and previous unreported use of other drugs.

In conclusion, we identified three distinct subtypes based on progression patterns of brain morphology. More progressed disease stages were found in TRS. The GP-CX type reflected an earlier stage of disease, but otherwise the subtypes did not show any relationship with clinical characteristics. Current findings provide new knowledge that may be relevant to the neural basis of TRS and, in so doing, lead to clinically useful personalized biomarkers.

Declarations

Acknowledgements

This study was supported by Japan Society for the Promotion of Science (18H02755, 22H03002), Takeda Science Foundation, Watanabe Foundation, Uehara Memorial Foundation, Inokashira Hospital Research Foundation (SN), Ontario Mental Health Foundation (OMHF) Type A grant (AGG) and by Canadian Institutes of Health Research (CIHR) Grant Nos. MOP-142493 (AGG, PG, GR) and MOP-141968 (AGG).

Conflict of interest

SN has received grants from Japan Society for the Promotion of Science (18H02755), Japan Agency for Medical Research and development (AMED), Japan Research Foundation for Clinical Pharmacology, Naito Foundation, Takeda Science Foundation, Uehara Memorial Foundation, and Daiichi Sankyo Scholarship Donation Program within the past three years. SN has also received research support, manuscript fees or speaker's honoraria from Dainippon Sumitomo Pharma, Meiji-Seika Pharma, Otsuka Pharmaceutical, Shionogi, and Yoshitomi Yakuhin within the past three years. GR has received research support from the Canadian Institutes of Health Research (CIHR), University of Toronto, and HLS Therapeutics Inc.

PG reports receiving research support from CIHR, OMHF, CAMH, CAMH Foundation, and an Academic Scholars Award from the Department of Psychiatry, University of Toronto. Y.N. has received a Grant-in-Aid

for Scientific Research (B) (21H02813) from the Japan Society for the Promotion of Science (JSPS), research grants from Japan Agency for Medical Research and Development (AMED), investigator-initiated clinical study grants from Teijin Pharma Ltd., and Inter Reha Co., Ltd. He also receives research grants from Japan Health Foundation, Meiji Yasuda Mental Health Foundation, Mitsui Life Social Welfare Foundation, Takeda Science Foundation, SENSHIN Medical Research Foundation, Health Science Center Foundation, Mochida Memorial Foundation for Medical and Pharmaceutical Research, Taiju Life Social Welfare Foundation, and Daiichi Sankyo Scholarship Donation Program. He has received speaker's honoraria from Dainippon Sumitomo Pharma, Mochida Pharmaceutical Co., Ltd., Yoshitomiyakuhin Co., Ltd., Qol Co., Ltd., Teijin Pharma Ltd., and Takeda Pharmaceutical Co., Ltd. within the past five years. He also receives equipment-in-kind support for an investigator-initiated study from Magventure Inc., Inter Reha Co., Ltd., Brainbox Ltd., and Miyuki Giken Co., Ltd. H.U. has received grants from Daiichi Sankyo, Eisai, Mochida, Otsuka, and Sumitomo Dainippon Pharma; speaker's fees from Eisai, Janssen, Lundbeck, Meiji Seika Pharma, Otsuka, and Sumitomo Dainippon Pharma; and advisory board fees from Lundbeck, Sumitomo Pharma and Boehringer Ingelheim Japan. FU has received fellowship grants from Discovery Fund, Nakatani Foundation, and the Canadian Institutes of Health Research (CIHR); manuscript fees from Dainippon Sumitomo Pharma; and consultant fees from VeraSci, and Uchiyama Underwriting within the past three years. MM has received speaker's honoraria from Biogen Japan, Byer Pharmaceutical, Daiichi Sankyo, Dainippon-Sumitomo Pharma, Demant Japan, Eisai, Eli Lilly, Fuji Film RI Pharma, Hisamitsu Pharmaceutical, H.U. Frontier, Janssen Pharmaceutical, Mochida Pharmaceutical, MSD, Mylan EPD, Nippon Chemipher, Novartis Pharma, Ono Yakuhin, Otsuka Pharmaceutical, Pfizer, Shionogi, Takeda Yakuhin, Teijin Pharma, and Viatris within the past three years.

References

1. Lieberman JA, First MB. Psychotic Disorders. *The New England journal of medicine* 2018; **379**(3): 270–280.
2. Derks EM, Allardyce J, Boks MP, Vermunt JK, Hijman R, Ophoff RA *et al.* Kraepelin was right: a latent class analysis of symptom dimensions in patients and controls. *Schizophr Bull* 2012; **38**(3): 495–505.
3. Palaniyappan L, Marques TR, Taylor H, Handley R, Mondelli V, Bonaccorso S *et al.* Cortical folding defects as markers of poor treatment response in first-episode psychosis. *JAMA Psychiatry* 2013; **70**(10): 1031–1040.
4. Wada M, Noda Y, Iwata Y, Tsugawa S, Yoshida K, Tani H *et al.* Dopaminergic dysfunction and excitatory/inhibitory imbalance in treatment-resistant schizophrenia and novel neuromodulatory treatment. *Mol Psychiatry* 2022; **27**(7): 2950–2967.
5. Beck K, McCutcheon R, Bloomfield MA, Gaughran F, Reis Marques T, MacCabe J *et al.* The practical management of refractory schizophrenia–the Maudsley Treatment REview and Assessment Team service approach. *Acta Psychiatr Scand* 2014; **130**(6): 427–438.

6. Kennedy JL, Altar CA, Taylor DL, Degtiar I, Hornberger JC. The social and economic burden of treatment-resistant schizophrenia: a systematic literature review. *Int Clin Psychopharmacol* 2014; **29**(2): 63–76.
7. Zugman A, Gadelha A, Assuncao I, Sato J, Ota VK, Rocha DL *et al.* Reduced dorso-lateral prefrontal cortex in treatment resistant schizophrenia. *Schizophr Res* 2013; **148**(1–3): 81–86.
8. Nakajima S, Takeuchi H, Plitman E, Fervaha G, Gerretsen P, Caravaggio F *et al.* Neuroimaging findings in treatment-resistant schizophrenia: A systematic review: Lack of neuroimaging correlates of treatment-resistant schizophrenia. *Schizophr Res* 2015; **164**(1–3): 164–175.
9. Itahashi T, Noda Y, Iwata Y, Tarumi R, Tsugawa S, Plitman E *et al.* Dimensional distribution of cortical abnormality across antipsychotics treatment-resistant and responsive schizophrenia. *NeuroImage Clinical* 2021; **32**: 102852.
10. Voineskos AN, Foussias G, Lerch J, Felsky D, Remington G, Rajji TK *et al.* Neuroimaging evidence for the deficit subtype of schizophrenia. *JAMA Psychiatry* 2013; **70**(5): 472–480.
11. Nenadic I, Yotter RA, Sauer H, Gaser C. Patterns of cortical thinning in different subgroups of schizophrenia. *Br J Psychiatry* 2015; **206**(6): 479–483.
12. Chand GB, Dwyer DB, Erus G, Sotiras A, Varol E, Srinivasan D *et al.* Two distinct neuroanatomical subtypes of schizophrenia revealed using machine learning. *Brain : a journal of neurology* 2020; **143**(3): 1027–1038.
13. van Haren NE, Schnack HG, Cahn W, van den Heuvel MP, Lepage C, Collins L *et al.* Changes in cortical thickness during the course of illness in schizophrenia. *Arch Gen Psychiatry* 2011; **68**(9): 871–880.
14. Cobia DJ, Smith MJ, Wang L, Csernansky JG. Longitudinal progression of frontal and temporal lobe changes in schizophrenia. *Schizophr Res* 2012; **139**(1–3): 1–6.
15. Demjaha A, Lappin JM, Stahl D, Patel MX, MacCabe JH, Howes OD *et al.* Antipsychotic treatment resistance in first-episode psychosis: prevalence, subtypes and predictors. *Psychol Med* 2017; **47**(11): 1981–1989.
16. Bozzatello P, Bellino S, Rocca P. Predictive Factors of Treatment Resistance in First Episode of Psychosis: A Systematic Review. *Front Psychiatry* 2019; **10**: 67.
17. Bzdok D, Meyer-Lindenberg A. Machine Learning for Precision Psychiatry: Opportunities and Challenges. *Biol Psychiatry Cogn Neurosci Neuroimaging* 2018; **3**(3): 223–230.
18. Dwyer DB, Falkai P, Koutsouleris N. Machine Learning Approaches for Clinical Psychology and Psychiatry. *Annu Rev Clin Psychol* 2018; **14**: 91–118.
19. Young AL, Marinescu RV, Oxtoby NP, Bocchetta M, Yong K, Firth NC *et al.* Uncovering the heterogeneity and temporal complexity of neurodegenerative diseases with Subtype and Stage Inference. *Nat Commun* 2018; **9**(1): 4273.
20. Eshaghi A, Young AL, Wijeratne PA, Prados F, Arnold DL, Narayanan S *et al.* Identifying multiple sclerosis subtypes using unsupervised machine learning and MRI data. *Nat Commun* 2021; **12**(1): 2078.

21. Vogel JW, Young AL, Oxtoby NP, Smith R, Ossenkoppele R, Strandberg OT *et al.* Four distinct trajectories of tau deposition identified in Alzheimer's disease. *Nat Med* 2021; **27**(5): 871–881.
22. Young AL, Bocchetta M, Russell LL, Convery RS, Peakman G, Todd E *et al.* Characterizing the Clinical Features and Atrophy Patterns of MAPT-Related Frontotemporal Dementia With Disease Progression Modeling. *Neurology* 2021; **97**(9): e941-e952.
23. Tarumi R, Tsugawa S, Noda Y, Plitman E, Honda S, Matsushita K *et al.* Levels of glutamatergic neurometabolites in patients with severe treatment-resistant schizophrenia: a proton magnetic resonance spectroscopy study. *Neuropsychopharmacology* 2020; **45**(4): 632–640.
24. Iwata Y, Nakajima S, Plitman E, Caravaggio F, Kim J, Shah P *et al.* Glutamatergic Neurometabolite Levels in Patients With Ultra-Treatment-Resistant Schizophrenia: A Cross-Sectional 3T Proton Magnetic Resonance Spectroscopy Study. *Biological psychiatry* 2019; **85**(7): 596–605.
25. Kim J, Plitman E, Iwata Y, Nakajima S, Mar W, Patel R *et al.* Neuroanatomical profiles of treatment-resistance in patients with schizophrenia spectrum disorders. *Prog Neuropsychopharmacol Biol Psychiatry* 2020; **99**: 109839.
26. Ochi R, Tarumi R, Noda Y, Tsugawa S, Plitman E, Wada M *et al.* Frontostriatal Structural Connectivity and Striatal Glutamatergic Levels in Treatment-Resistant Schizophrenia: An Integrative Analysis of DTI and 1H-MRS. *Schizophrenia Bulletin Open* 2020; **1**(1).
27. Shah P, Plitman E, Iwata Y, Kim J, Nakajima S, Chan N *et al.* Glutamatergic neurometabolites and cortical thickness in treatment-resistant schizophrenia: Implications for glutamate-mediated excitotoxicity. *J Psychiatr Res* 2020; **124**: 151–158.
28. Association AP. *DSM-IV Diagnostic and Statistical Manual of Mental Disorders, 4th ed.* American Psychiatric Press: Washington, DC, 1994.
29. Kay SR, Fiszbein A, Opler LA. The positive and negative syndrome scale (PANSS) for schizophrenia. *Schizophr Bull* 1987; **13**(2): 261–276.
30. Busner J, Targum SD. The clinical global impressions scale: applying a research tool in clinical practice. *Psychiatry (Edgmont)* 2007; **4**(7): 28–37.
31. Howes OD, McCutcheon R, Agid O, de Bartolomeis A, van Beveren NJ, Birnbaum ML *et al.* Treatment-Resistant Schizophrenia: Treatment Response and Resistance in Psychosis (TRRIP) Working Group Consensus Guidelines on Diagnosis and Terminology. *The American journal of psychiatry* 2017; **174**(3): 216–229.
32. Sheehan DV, Lecrubier Y, Sheehan KH, Amorim P, Janavs J, Weiller E *et al.* The Mini-International Neuropsychiatric Interview (M.I.N.I.): the development and validation of a structured diagnostic psychiatric interview for DSM-IV and ICD-10. *J Clin Psychiatry* 1998; **59 Suppl 20**: 22–33;quiz 34–57.
33. van Erp TG, Hibar DP, Rasmussen JM, Glahn DC, Pearlson GD, Andreassen OA *et al.* Subcortical brain volume abnormalities in 2028 individuals with schizophrenia and 2540 healthy controls via the ENIGMA consortium. *Mol Psychiatry* 2016; **21**(4): 547–553.
34. van Erp TGM, Walton E, Hibar DP, Schmaal L, Jiang W, Glahn DC *et al.* Cortical Brain Abnormalities in 4474 Individuals With Schizophrenia and 5098 Control Subjects via the Enhancing Neuro Imaging

Genetics Through Meta Analysis (ENIGMA) Consortium. *Biological psychiatry* 2018; **84**(9): 644–654.

35. Kim E, Howes OD, Veronese M, Beck K, Seo S, Park JW *et al.* Presynaptic Dopamine Capacity in Patients with Treatment-Resistant Schizophrenia Taking Clozapine: An [(18)F]DOPA PET Study. *Neuropsychopharmacology* 2017; **42**(4): 941–950.
36. Okada N, Fukunaga M, Yamashita F, Koshiyama D, Yamamori H, Ohi K *et al.* Abnormal asymmetries in subcortical brain volume in schizophrenia. *Mol Psychiatry* 2016; **21**(10): 1460–1466.
37. Ochi R, Plitman E, Patel R, Tarumi R, Iwata Y, Tsugawa S *et al.* Investigating structural subdivisions of the anterior cingulate cortex in schizophrenia, with implications for treatment resistance and glutamatergic levels. *J Psychiatry Neurosci* 2022; **47**(1): E1-E10.
38. Ueno F, Nakajima S, Iwata Y, Honda S, Torres-Carmona E, Mar W *et al.* Gamma-aminobutyric acid (GABA) levels in the midcingulate cortex and clozapine response in patients with treatment-resistant schizophrenia: A proton magnetic resonance spectroscopy ((1) H-MRS) study. *Psychiatry Clin Neurosci* 2022.
39. Palaniyappan L, Sabesan P, Li X, Luo Q. Schizophrenia Increases Variability of the Central Antioxidant System: A Meta-Analysis of Variance From MRS Studies of Glutathione. *Front Psychiatry* 2021; **12**: 796466.

Figures

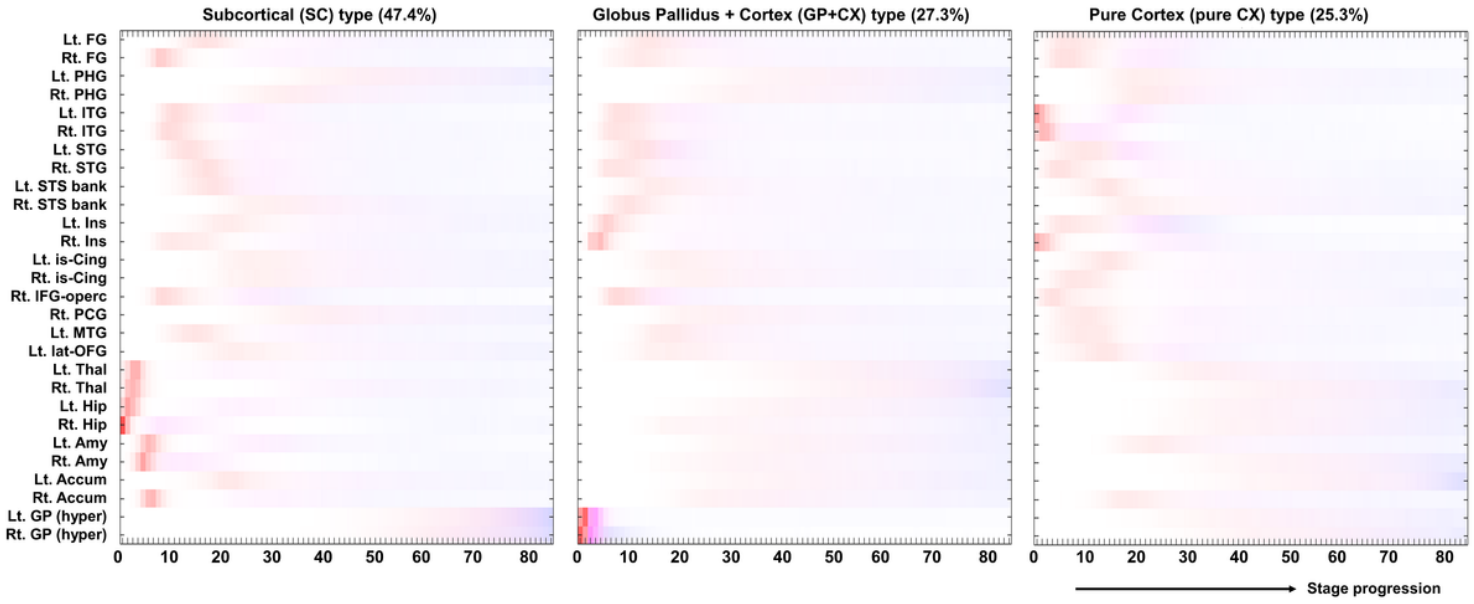

Figure 1

Estimated three patterns of brain morphological disease progression in schizophrenia, namely 1) subcortical volume reduction (SC) type, in which volume reduction of subcortical structures occurs first and moderate cortical thinning follows, 2) globus pallidus hypertrophy and cortical thinning (GP-CX) type, in which globus pallidus hypertrophy initially occurs followed by progressive cortical thinning, and 3)

cortical thinning (pure CX) type, in which thinning of the insular and lateral temporal lobe cortices primarily happens.

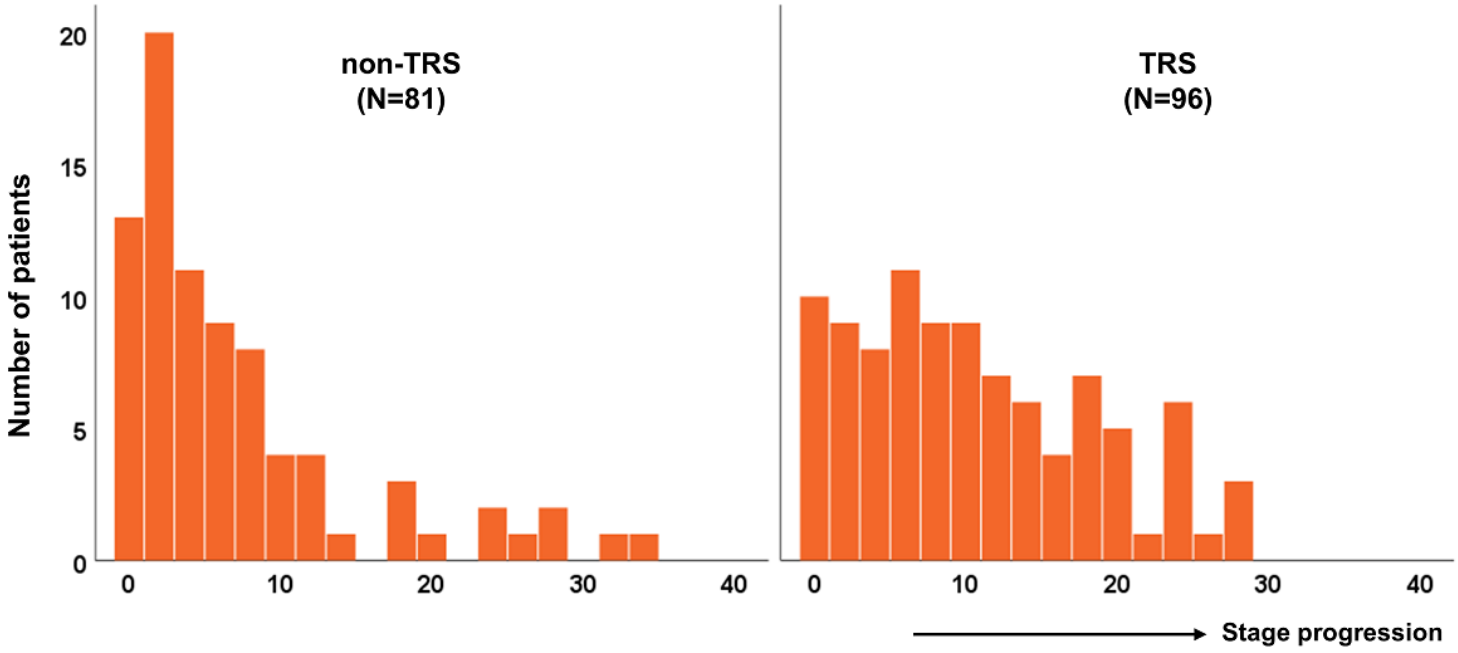

Figure 2

Histogram of stage progressions between non-TRS and TRS.

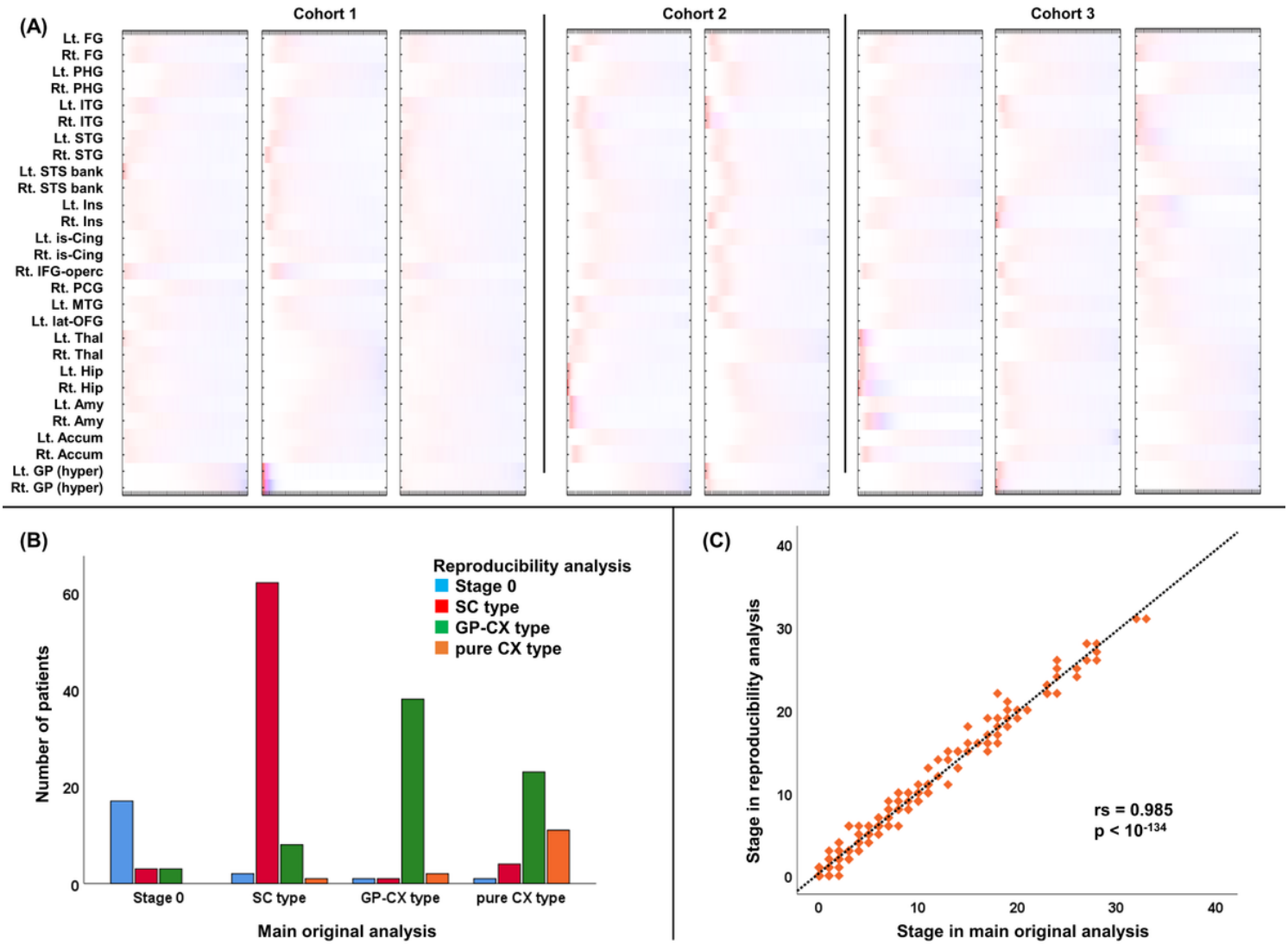

Figure 3

Reproducibility analysis by analyzing each cohort separately. (A) Subtype and staging results of each cohort. (B) Subtype classification between main original analysis and reproducibility analysis. (C) Correlation of stage progressions between main original analysis and reproducibility analysis.

Supplementary Files

This is a list of supplementary files associated with this preprint. Click to download.

- SupplementaryTableS1.pdf